Evaluation of Total and Corneal Wavefront High Order Aberrations for the Detection of Forme Fruste Keratoconus

Alain Saad and Damien Gatinel

Purpose. To investigate the application of anterior corneal and ocular aberrations in detecting mildly ectatic corneas.

Methods. This study retrospectively reviewed the data of 220 eyes separated into three groups by the NIDEK Corneal Navigator System automated corneal classification software: normal (N) ($n = 123$); forme fruste keratoconus (N topography with contralateral KC) ($n = 34$); and KC ($n = 63$). Anterior corneal and ocular aberrations were obtained with the optical path difference scan and compared using a Kruskal-Wallis test. Evaluation of these data to discriminate between the three groups was assessed using a Receiver-Operating Characteristic curve analysis.

Results. Corneal and ocular tilt, vertical coma, and trefoil were significantly different in the FFKC as compared with the N group. The discriminant functions between the FFKC and the N group, and between the KC and the N group reached an area under the receiver operating characteristic curve of 0.98 and 0.96, respectively.

Conclusion. Indices generated from corneal and ocular wavefront can identify very mild forms of ectasia that may be undetected by Placido-based neural network programs. (*Invest Ophthalmol Vis Sci.* 2012;53:2978–2992) DOI:10.1167/iovs.11-8803

Ectasia remains the most dreaded complication after refractive surgery. Hence, there is great interest in attempting to preoperatively identify patients at risk for this complication.[1–6] Similarity with ectatic corneas (keratoconus [KC]) or pellucid marginal corneal degeneration) is the main independent risk factor.[1,3,7] A major goal in preventing post-laser in situ keratomileusis ectasia is to detect corneas with subclinical keratoconus in its earliest and mildest form. Clinical keratoconus can be reliably detected with corneal topography or slit lamp examination. However, although detection of subclinical keratoconus in its earliest stages has been extensively explored, definitive criteria remain elusive. Several terms have been employed to describe this condition, including subclinical keratoconus, keratoconus suspect (KCS), and forme fruste keratoconus (FFKC). Initially, the term KCS was introduced to describe videokeratography that the clinician considered high risk for progression to KC based solely on subjective impression. The use of quantitative videokeratography-derived indices represents a more reproducible way of quantifying KC and its early phenotypes and reduces the complexity of proper classification.[8–11] This approach allows the determination of an accurate transition from normal to suspect and subsequent KC.[12,13].Thus, the term KCS should be reserved for corneas that exhibit topographically detectable features of subclinical keratoconus based on computerized segregation analysis with Placido topography.

Conversely, Klyce[14] proposed the term forme fruste keratoconus for corneas that exhibit subtle topographic characteristics suggestive of an early subclinical keratoconus that is not pronounced enough to reach the threshold of keratoconus suspicion with automated classification. For example, a topographic pattern of an asymmetric bowtie with a skewed radial axis is suggestive of subclinical keratoconus. Depending on the relative importance of each topographic feature, positive automated detection (keratoconus suspect cornea) or a negative automated classification may result. However, the negative classification may not indicate the absence of an early form of subclinical keratoconus. Similarly, an abnormal inferior/superior value may merely represent a false positive, and is not necessarily an indicator of a keratoconic subtype. A recent study found that indices generated from corneal thickness and curvature measurements over the entire cornea and calculations of percentage of thickness increase and percentage of anterior and posterior curvature variation from the thinnest point to the periphery can identify very mild forms of KC undetected by Placido-based neural network.[5] This approach suggests that the addition of elevation and tomography data may allow for better sensitivity and specificity for the detection of FFKC than Placido data alone.[5,15]

Studies have shown that wavefront technology may also be a useful adjunct to topography for diagnosing keratoconus.[16–18] Therefore, the combination of videokeratography and wavefront analysis may help define keratoconic subtypes and increase the sensitivity and specificity for early detection of subclinical keratoconus.

KC is an asymmetric[19] progressive disorder that ultimately affects both eyes. The incidence of "true" unilateral KC is very low.[20,21] Some studies suggest that with long-term follow-up, patients with unilateral KC will show signs of keratoconus in the fellow eye.[21,22] Therefore, the contralateral topographically normal eye of a patient with unilateral KC is the mildest and earliest form of the disease[14,23,24] and corresponds to the proposed definition of forme fruste keratoconus. Though the possibility exists of a small number of cases where KC may not develop in the contralateral eyes, one must be cognizant of the fact that the genetic makeup is the same in both eyes.[25–27] Therefore, the fellow "unaffected" eye of a unilateral KC patient should be considered susceptible for developing ectasia if it undergoes laser in situ keratomileusis.

In their innovative study, Buhren et al. found that anterior corneal surface aberrations can be used for the detection of subclinical keratoconus, specifically in patients with an eye

From the Rothschild Foundation and the [2]Center for Expertise and Research in Optics for Clinicians (CEROC), Paris, France.

Submitted for publication October 15, 2011; revised February 2, 2012; accepted February 26, 2012.

Disclosure: **A. Saad**, Acufocus Inc (C) and Technolas Perfect Vision (C); **D. Gatinel**, Technols Perfect Vision (C)

Corresponding author: Damien Gatinel, Fondation Ophtalmologique Adolphe de Rothschild, 25, Rue Manin 75019, Paris, France. gatinel@gmail.com, dralainsaad@gmail.com.

that appears subjectively normal but has diagnosed KC in the contralateral eye.[16,17]

Data suggest that patients with objectively Placido normal eyes with contralateral KC[5] represent a unique opportunity to investigate detection of the mildest form of the disease. This study compared the ocular and anterior corneal wavefront data of FFKC eyes, KC eyes, and normal eyes. An important component of the study was the comparison of discriminant functions constructed from the analysis of the anterior corneal and ocular wavefront data in order to improve the sensitivity and specificity of discriminant analysis for the detection of at-risk corneas.

Methods

Patients

This study adhered to the tenets of the Declaration of Helsinki and Institutional Review Board approval was obtained. Two hundred and twenty eyes of 142 patients from the Department of Ophthalmology of the Rothschild Foundation (Paris, France) were included and separated into three groups: normal, FFKC, and KC group.

Segregation of the three groups was based on the results of the NIDEK Corneal Navigator automated corneal classification software in the OPD-Scan (NIDEK Co. Ltd., Gamagori, Japan), which uses an artificial intelligence technique to train a computer neural network to recognize specific classifications of corneal topography. The NCN first calculates various indices representing corneal shape characteristics. The indices are then used by the NCN to score the measurement's similarity to nine clinical classification types: normal, astigmatism, suspected keratoconus, keratoconus, pellucid marginal degeneration, postkeratoplasty, myopic refractive surgery, hyperopic refractive surgery, and unclassified variation.

These diagnostic results are estimated based on the relationship between the corneal indices and cases. The percentage of similarity is indicated for each diagnostic condition; the value varies from 0% to 99%. The result for each topographic condition is independent from other categories.

The FFKC group was composed of 34 topographically normal eyes of patients with KC in the other eye (representative topographies of this group are shown in the Appendix). In these patients, the NCN indicated a null score similarity to KCS and KC for the selected eyes and a non-null score similarity to KC for the contralateral eyes. The contralateral eyes also had frank KC evident on corneal topography.

Patients with a documented history of compulsive bilateral eye rubbing or a chronic habit of abnormal unilateral rubbing were excluded. To be included in the study, valid anterior corneal and ocular aberration data measured with the OPD-Scan through a 5-mm pupil were required.

The normal (N) group was composed of 123 eyes of 69 patients who had undergone LASIK with 3 years' follow-up, with no postoperative complications such as ectasia. Only the preoperative topographies were considered in the N group. Eyes in the N group had a score of 99% similarity to normality using the NCN analysis and Orbscan IIz (Technolas Perfect Vision, Munich, Germany) data did not reveal topographic patterns suggestive of KCS, such as focal or inferior steepening of the cornea or central keratometry greater than 47.0 D.

The KC group included 63 eyes of 39 patients that had frank keratoconus diagnosed by an experienced corneal specialist on the basis of clinical and topographic signs (with a positive similarity score to KC indicated by the NCN). No contact lens wear for at least 4 weeks (rigid CL) or 2 weeks (soft CL), and no signs or symptoms of dry eye were present in the included patients.

Wavefront and Corneal Aberrations

The OPD-Scan (NIDEK) aberrometer is a combined automated retinoscopy and Placido disk videokeratoscope. The measurement details have been previously described.[28–30] All OPD-Scan measurements were acquired in a dark examination room (2.2 Lux), after 2 minutes of dark adaptation, were repeated three times consecutively, then averaged. Total and corneal wavefront aberrations were reconstructed using a sixth order Zernike polynomial decomposition for a 5-mm pupil, centered on the vertex normal.

Enantiomorphism was neutralized by inverting the sign of the mirror-symmetric coefficients of the left eyes as shown in Eqs. 1 and 2.

$$\text{for all } C_n^m \text{ if } n \text{ is even and } m < 0 => C_n^m = -(C_n^m) \quad (1)$$

$$\text{for all } C_n^m \text{ if } n \text{ is odd and } m > 0 => C_n^m = -(C_n^m) \quad (2)$$

The magnitudes of coma, trefoil, and spherical aberration were also calculated, for corneal and ocular terms, respectively. The total root mean square for coma aberration (coma RMS) associated the following aberrations (corneal versus ocular): $7\text{th} = Z_3^{-1}$; $8^{\text{th}} = Z_3^{1}$; $17\text{th} = Z_5^{-1}$; $18\text{th} = Z_5^{1}$ terms). The total RMS for trefoil aberration (trefoil RMS) associated the following aberrations (corneal versus ocular): $6^{\text{th}} = Z_3^{-3}$; $9\text{th} = Z_3^{3}$; $16\text{th} = Z_5^{-3}$; $19\text{th} = Z_5^{3}$ terms. The total RMS for spherical aberration (spherical aberration RMS) associated the following aberrations (corneal versus ocular):$12\text{th} = Z_4^{0}$ and $24\text{th} = Z_6^{0}$ terms.

Statistical Analysis, Discriminant Analysis, and ROC curve

All numerical results were entered into a database, and statistical analyses were performed (XLSTAT 2010 statistical analysis software; Addinsoft, New York, NY) with the Kruskal-Wallis test followed by a Weaver-Dunn procedure for multiple nonparametric comparisons and a Bonferroni correction to maintain a global level of $P < 0.05$.

Discriminant analysis was used to determine the group of an observation based on a set of variables obtained from the anterior corneal wavefront and from the ocular wavefront. On the basis of the N and FFKC groups, the discriminant analysis constructs a set of linear functions of the variables, known as discriminant functions, such as

$$L = b_1x_1 + b_2x_2 + b_nx_n + c \quad (3)$$

where b is a discriminant coefficient, x is an input variable, and c is a constant. The following discriminant functions were generated:

1. FC: Zernike coefficients and RMS of the anterior corneal wavefront;
2. FT: Zernike coefficients and RMS of the ocular wavefront; and
3. FCT: Zernike coefficients and RMS of the anterior corneal and ocular wavefront.

Thus, for the building of a discriminant function based on anterior corneal and ocular wavefront, 34 FFKC eyes and 123 N eyes were considered. The discriminant functions can be used to predict the class of a new observation with unknown class.

Receiver operating characteristic curves were plotted to obtain critical values that allow classification with maximum accuracy. For the output values of the discriminant functions tested, the area under the ROC curve—sensitivity [true positive / (true positive + false negative)]; specificity [true negative / (true negative false positive)]; accuracy [(true positive + true negative) / total number of cases]; and cutoff value—were calculated and compared.

Results

Table 1 presents the demographic data for each group. The mean age was not significantly different between groups ($P > 0.05$, all comparisons). The mean sphere was significantly higher in the N group compared with the FFKC group ($P < 0.001$) and the mean cylinder was significantly higher in the KC group compared with the N and FFKC group ($P < 0.001$).

Ocular Wavefront Data

The ocular wavefront data was significantly different between the N group and the KC group for the following Zernike coefficients and RMS values: ZO_1^{-1}; ZO_1^{1}; ZO_3^{-3}; ZO_3^{-1};

Table 1. Demographic Characteristics of Each Group

	Normal	FFKC	KC
Patients (n)	69	34	39
Eyes (n)	123	34	63
Age (mean ± SD)	34.7 ± 8.2	33.9 ± 12.4	33.0 ± 8.0
Sphere (D) [Range]	−4.6 ± 3.0 [−10.75; 4.75]	−1.5 ± 2.4 [−8.75; 0.75]	−3.3 ± 3.9 [−13.5; +2.50]
Cylinder (D) [Range]	−0.75 ± 0.75 [−3.75; 0]	−0.69 ± 0.69 [−3.25; 0]	−2.63 ± 1.95 [−8.50; 0]

ZO_3^1; ZO_4^{-4}; ZO_4^{-2}; ZO_4^0; ZO_4^4; ZO_5^{-3}; ZO_6^{-2}; coma RMS; trefoil RMS; and spherical aberration RMS. Table 2 presents the statistically different parameters between the N group and the FFKC group.

Corneal Wavefront Data

The corneal wavefront data was statistically different between the N group and the KC group for the following ZC and RMS values: ZC_1^{-1}; ZC_1^1; ZC_2^{-2}; ZC_4^0; ZC_3^{-3}; ZC_3^{-1}; ZC_3^1; ZC_4^{-4}; ZC_4^{-2}; ZC_4^0; ZC_4^2; ZC_4^4; ZC_5^{-5}; ZC_5^{-3}; ZC_5^{-1}; ZC_5^1; coma RMS; trefoil RMS; and spherical aberration RMS. Table 2 presents the statistically different parameters between the N group and the FFKC group.

Discriminant Analysis and ROC Curves

The formulas for all discriminant functions are included in the Appendix. The functions were derived from N and FFKC Zernike coefficients and RMS values and their output values were tested to differentiate between the N and FFKC groups, and the N and KC groups. The output values of the discriminant function were significantly different between the three groups ($P < 0.0001$; see Table 3). The function DA 23 consisted of the same corneal Zernike reported by Buhren et al.[16] (ZC_1^{-1}; ZC_2^2; ZC_3^3; ZC_4^0; ZC_5^{-3}; ZC_5^1; ZC_6^4; ZC_6^6) with ZC_6^6 having the highest discriminant coefficient (1.549). The function FC was derived from the anterior corneal Zernike coefficients and RMS values and consisted of: ZC_1^{-1}; ZC_2^0; ZC_2^2; ZC_3^{-3}; ZC_3^3; ZC_4^{-4}; ZC_4^{-2}; ZC_4^2; ZC_5^{-3}; ZC_5^{-1}; ZC_6^4; ZC_6^6—in addition to coma RMS and trefoil RMS—with ZC_6^6 having the highest discriminant coefficient (2.297). The function FT was derived from the ocular wavefront Zernike coefficient and consisted of ZO_1^{-1}; ZO_1^1; ZO_3^{-3}; ZO_3^{-1}; ZO_3^1; ZO_3^3; ZO_4^{-4}; ZO_4^{-2}; ZO_4^0; ZO_5^{-3}; ZO_6^{-2}; ZO_6^0; ZO_6^4; and coma RMS, with ZO_6^4 having the highest discriminant coefficient (1.063). The function FCT was derived from the corneal and ocular corneal Zernike coefficients and RMS values, with ZO_6^6 having the highest discriminant coefficient (2.611).

The discriminative ability of the individual Zernike coefficients and RMS values that were statistically different between the N group and the FFKC group are reported in Table 4. Ocular vertical coma (ZO_3^{-1}) had the highest discriminative ability between the N group and the FFKC group (AUROC = 0.831; sensitivity = 72%; specificity = 81%). All the other individual Zernike coefficients or RMS values had an AUROC of less than 0.8 for differentiating between the N group and the FFKC group. For the distinction between the N and KC group, corneal and ocular tilt (ZC_1^{-1}; ZO_1^{-1}), corneal and ocular vertical coma (ZC_3^{-1}; ZO_3^{-1}); and coma and trefoil RMS values reached an AUROC of more than 0.96 with the corneal tilt (ZC_1^{-1}) having the best sensitivity (98%) and specificity (100%). The AUROC for the distinction between the N and KC group were not available for ZC_3^3, ZO_3^3, and ZO_6^0 because these parameters were not significantly different between the two groups.

For the distinction between the N group and the FFKC, output values of the FCT function based on corneal and ocular wavefront Zernike reached an AUROC of 0.985, a sensitivity of 91%, a specificity of 94%, and an accuracy of 93% (Table 4). The other functions had an accuracy comprised between 80% and 86%.

For the distinction between the N group and the KC group, all the output values of the discriminant functions yielded a sensitivity and a specificity higher than 90%. In Fig. 1, the ROC curves of all the discriminant functions are displayed graphically.

Discussion

Many investigators have tried to define specific and objective topographic criteria in order to detect very early or mild forms of subclinical keratoconus.[9,31] This has become particularly relevant for ruling out early keratoconus when screening candidates for refractive surgery to reduce the risk of ectasia.

Table 2. Wavefront Parameters with Statistically Significant Differences between N Group and FFKC Group (Mean ± SD in microns)

	Normal	FFKC	KC
Ocular aberrations			
ZO_1^{-1}	0.022 ± 0.217	−0.179 ± 0.254	−2.006 ± 1.434
ZO_3^{-1}	0.008 ± 0.087	−0.100 ± 0.091	−0.747 ± 0.518
ZO_3^3	0.018 ± 0.187	−0.070 ± 0.127	0.012 ± 0.477
ZO_6^0	0.007 ± 0.042	0.110 ± 0.020	0.019 ± 0.039
Corneal aberrations			
ZC_1^{-1}	0.026 ± 0.271	−0.334 ± 0.335	−4.309 ± 2.608
ZC_3^{-1}	−0.016 ± 0.117	−0.139 ± 0.129	−1.525 ± 0.894
ZC_3^3	−0.011 ± 0.065	−0.106 ± 0.095	−0.059 ± 0.345
Coma RMS	0.118 ± 0.096	0.199 ± 0.094	1.712 ± 1.006
Trefoil RMS	0.110 ± 0.105	0.172 ± 0.077	0.545 ± 0.306

Table 3. Output Values of the Discriminant Functions ($P < 0.001$ between the groups)

	N	FFKC	KC
DA23 (mean ± SD)			
[Range]	−0.40 ± 0.88 [−2.82; 2.28]	1.45 ± 1.35 [−1.32; 3.72]	10.29 ± 7.36 [0.17; 30.53]
FC	−0.54 ± 0.75 [−2.46; 1.67]	1.96 ± 1.62 [−1.00; 4.87]	15.81 ± 11.56 [−4.53; 50.17]
FT	−0.47 ± 0.90 [−3.04; 2.28]	1.79 ± 1.32 [−0.61; 4.44]	15.94 ± 12.70 [−2.55; 54.85]
FCT	−0.68 ± 0.88 [−2.45; 1.45]	2.60 ± 1.45 [0.34; 5.38]	17.28 ± 15.06 [−6.01; 74.13]

To detect these corneas before any clinical and known topographical manifestation of the pathology, the study of contralateral topographically "normal" eyes of keratoconic patients seems reasonable. For example, keratoconus is a bilateral, progressive asymmetric disease; hence, it is legitimate to postulate that the apparently normal corneas of patients with keratoconus in one eye may contain some indices that remain undetected by current automated topography detection software.

The association of keratoconus and eye rubbing is a frequent clinical observation.[32,33] Vigorous rubbing may expose the thinner or weakened cone apex to high intraocular pressure and the attendant distention that may promote ectasia.[34,35] Cases of unilateral keratoconus due to vigorous chronic unilateral eye rubbing have been reported.[36,37] However, in the current study, patients with documented, compulsive unilateral eye rubbing were excluded from the FFKC group.

The differences in corneal HOA between the N group and the FFKC group were comparable to those found by Buhren et al. (Table 2). The corneal tilt (ZC_1^{-1}) and the corneal vertical coma (ZC_3^{-1}) were significantly more negative in the FFKC group compared with the N group. However, contrary to Buhren et al., this study found a magnitude of coma RMS in the FFKC group (0.199 ± 0.094 microns) higher than the N group (0.118 ± 0.096 microns) and lower than the KC group (1.712 ± 1.006 microns). This is expected as the FFKC cornea corresponds to a very early pathological state in the natural history of keratoconus.

Significantly more negative corneal trefoil (ZC_3^3) was found in the FFKC group compared with the N group; however, there was no difference between the N group and the KC group. This can be explained by the large standard deviation of the corneal trefoil value (−0.059 ± 0.345 microns) in the KC group, where it varies from highly negative to highly positive values, leading to a mean value approaching zero. However, there was a significant difference between the three groups in the RMS of corneal trefoil, as this RMS value corresponds to the overall magnitude of the trefoil aberration, regardless of the orientation.

The ocular tilt (ZO_1^{-1}), vertical coma (ZO_3^{-1}), and trefoil (ZO_3^3) Zernike coefficients were also significantly higher in the FFKC group compared with the N group. However, the RMS values of ocular coma and ocular trefoil were not different between the two groups (approaching significance for coma, $P = 0.027$ with a Bonferroni correction leading a threshold P value of 0.0167 for statistical significance). This might partly be due to internal aberrations compensating for the corneal aberrations generated by the FFKC cornea.[38] Additionally, the possibility exists that there is a difference in the sensitivity of Placido and automated skiascopy technology. Subtle change in the corneal anterior surface may be detected with Placido technology, but undersampled, or smoothed during wavefront reconstruction.

In addition, the RMS value of ocular spherical aberration term (ZO_6^0) was significantly higher in the FFKC group compared with the N group; however, the ocular spherical aberration RMS was not significantly different between the N group and the KC group. Ocular and corneal tilt (ZO_1^{-1}, ZC_1^{-1}) and coma (ZO_3^{-1}, ZC_3^{-1}) individual Zernike coefficients, as well as the RMS of corneal coma and trefoil were able

Table 4. Results of ROC Analysis of Individual Zernike Coefficients and Discriminant Functions

	Cutoff value		AUROC		Sensitivity (%)		Specificity (%)		Accuracy (%)	
	N vs. FFKC	N vs. KC	N vs. FFKC	N vs. KC	N vs. FFKC	N vs. KC	N vs. FFKC	N vs. KC	N vs. FFKC	N vs. KC
Corneal aberrations										
ZC_1^{-1}	−0.185	−0.859	0.780	0.998	73	98	73	100	74	99
ZC_3^{-1}	−0.095	−0.426	0.792	0.978	71	97	78	100	77	99
ZC_3^3	−0.048	−0.048	0.796		71		73		73	
Coma RMS	0.157	0.257	0.778	0.988	71	98	80	99	78	99
Trefoil RMS	0.118	0.180	0.765	0.960	76	94	65	94	67	94
Ocular aberrations										
ZC_1^{-1}	−0.058	−0.552	0.766	0.981	78	94	65	100	68	98
ZC_3^{-1}	−0.065	−0.168	0.831	0.974	72	97	81	100	79	99
ZC_3^3	−0.013		0.672		69		61		63	
ZC_6^0	0.016		0.682		66		67		67	
Discriminant functions										
FC	0.214	1.667	0.912	0.972	82	95	87	100	86	98
FT	0.477	2.278	0.925	0.983	84	94	85	100	85	98
FCT	0.613	0.990	0.985	0.961	91	92	94	99	93	97
DA23	0.181	0.863	0.876	0.988	79	94	80	93	80	93

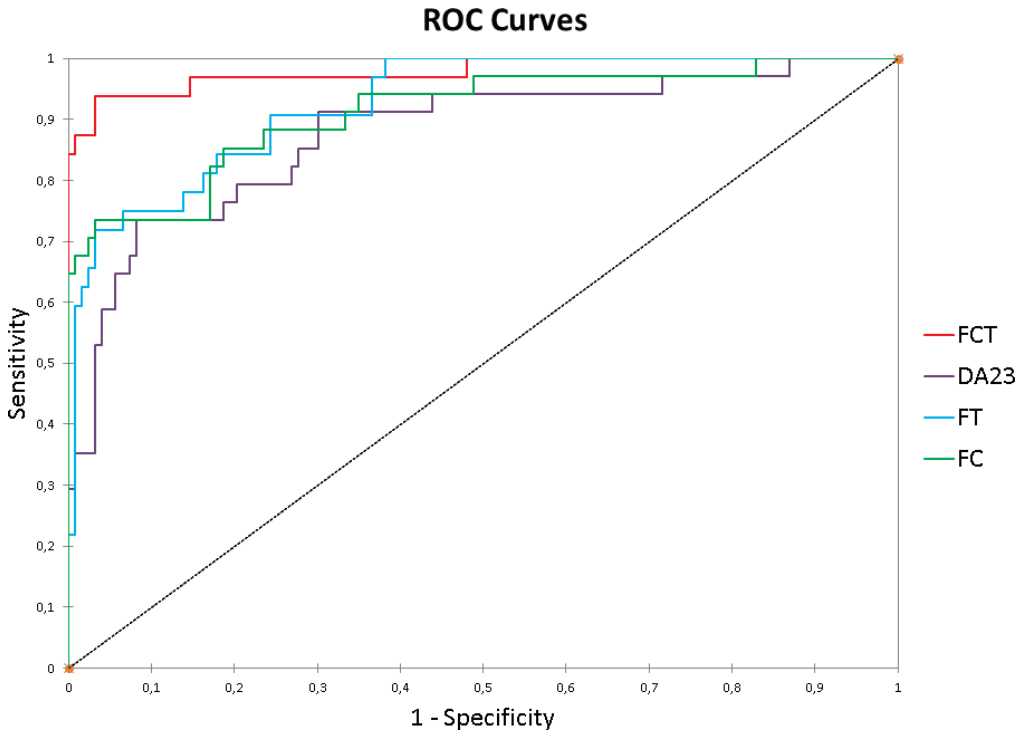

FIGURE 1. ROCs of the different function for discrimination between N group and FFKC group.

to differentiate between the N group and the KC group with good accuracy (>98% for all except RMS trefoil, 94%).

Higher levels of coma in KC eyes were previously reported and study findings concurs with previous literature.[18,39–41] Buhren et al.[16] also reported that corneal tilt and coma (Z_1^{-1}; Z_3^{-1}) values can be used to distinguish N from KC corneas with good accuracy (90.2% and 99.6%, respectively). However, the cutoff values of these aberrations between the N group and the KC group were not similar to our study. The cutoff value depended on the severity of the KC group under study and on the method of measurement of the aberrations. These two elements were different in the two studies and the difference in corneal aberrations measured or calculated with different instruments was reported.[42]

The accuracy of the corneal tilt (ZC_1^{-1}) and coma (ZC_3^{-1}) for the discrimination between N group and FFKC group was 74% and 77%, respectively. These values are much lower than those reported by Buhren et al.[16] between subjectively normal fellow eyes of KC and N corneas (92.7% and 95.4%, respectively). This difference in the ability of discrimination of corneal tilt and coma between the two studies is due to the fact that the current study group of objectively selected normal fellow eyes of KC (FFKC group) patients is the earliest identifiable stage of the disease.

In this study, the association of corneal (FC) or ocular (FT) Zernike coefficients or both (FCT) in discriminant functions reached good sensitivity and specificity in the diagnosis of FFKC (Table 4). The FC and FT results were quite similar and were able, with 14 variables, to discriminate the FFKC group from the N group with an accuracy of 86% and 85%, respectively. The association of corneal and ocular aberrations in one function including 22 variables gave the best sensitivity and specificity (91 and 94 % respectively, accuracy 93%). The discriminant analysis was conducted not only with Zernike coefficients but also with coma RMS, trefoil RMS, and spherical aberration RMS. This indicated that the Zernike terms that were used for calculating RMS were used twice in the function. Although independent variables should be generally used for discriminant analysis, some of the variables might be dependent. In this specific case, both the values of single Zernike terms and the magnitude of some Zernike vectors corresponding to groups of aberration terms of the same class (e.g., coma, trefoil, and spherical aberration) are important and present some discriminant ability.

These functions (FC, FT, and FCT) were built with input variables from the FFKC group and N group, but they were also able to discriminate between KC group and N group with good accuracy (between 97% and 98%). The ability of these functions to recognize KC—while they were constructed to identify FFKC—is a good indicator of the consistency of this method. In KC eyes, the accuracy and repeatability of the measurements is lower than in normal eyes.[43] This can lead to some aberrant values of Zernike terms in some KC eyes. As FCT include more Zernike terms, there is more risk that one aberrant value leads to a misclassification of the concerned examination. This can explain the slightly lower accuracy of the FCT function (97%) in comparison to the FC or FT (98%). A function was constructed with the same input variables as DA23 described by Buhren et al.,[16] who reported 96.7% accuracy. In this study, DA23 reached an accuracy of 80% for the detection of FFKC. The current study's FFKC group is likely more challenging and difficult to detect because it comprises eyes having the earliest form of the disease.

Interestingly, not all Zernike coefficients that were significantly different between the N group and the FFKC group were integrated in the discriminant functions. Corneal vertical coma was not included in the FC even if it was one of the best individual variables in discriminating between the N group and the FFKC group. The same finding was reported by Buhren et al.,[16] as DA23 function did not include vertical coma. The increase in corneal coma aberration measured in the FFKC group may be proportional to the physical asymmetry and

relative tilt of the slightly ectatic anterior corneal surface relative to the plane of the entrance pupil. Thibos et al. suggested a strong correlation between first-order terms (vertical and horizontal tilt) and third-order coma terms.[44] Thus, the inclusion of vertical coma in a function that already includes tilt did not bring any new information to the function because of the strong correlation between the two Zernike terms.

In conclusion, discriminant analysis using data obtained with combined corneal and ocular wavefront data enables the detection of early subclinical keratoconus that may not be detected by Placido-based topography analysis (FFKC) with a sensitivity and a specificity of 91% and 94%, respectively. The results of the present study are promising; however, the application of the Zernike method for automated detection of "at-risk corneas" warrants greater study in a larger sample size and the repeatability of the measurements have to be assessed. The limited sample size was due to the low incidence of patients with objective unilateral keratoconus (eyes with proven FFKC) and it represents the main drawback of the study. In the future, the combination of wavefront data and tomography data may provide a better approach for the detection of corneas susceptible to ectasia.

References

1. Binder PS. Risk factors for ectasia after LASIK. *J Cataract Refract Surg*. 2008;34:2010–2011.
2. Binder PS, Trattler WB. Evaluation of a risk factor scoring system for corneal ectasia after LASIK in eyes with normal topography. *J Refract Surg*. 2010;26:241–250.
3. Randleman JB, Trattler WB, Stulting RD. Validation of the Ectasia Risk Score System for preoperative laser in situ keratomileusis screening. *Am J Ophthalmol*. 2008;145:813–818.
4. Randleman JB, Woodward M, Lynn MJ, Stulting RD. Risk assessment for ectasia after corneal refractive surgery. *Ophthalmology*. 2008;115:37–50.
5. Saad A, Gatinel D. Topographic and tomographic properties of forme fruste keratoconus corneas. *Invest Ophthalmol Vis Sci*. 2010;51:5546–5555.
6. Saad A, Lteif Y, Azan E, Gatinel D. Biomechanical properties of keratoconus suspect eyes. *Invest Ophthalmol Vis Sci*. 2010; 51:2912–2916.
7. Saad A, Gatinel D. Bilateral corneal ectasia after laser in situ keratomileusis in patient with isolated difference in central corneal thickness between eyes. *J Cataract Refract Surg*. 36:1033–1035.
8. Schlegel Z, Hoang-Xuan T, Gatinel D. Comparison of and correlation between anterior and posterior corneal elevation maps in normal eyes and keratoconus-suspect eyes. *J Cataract Refract Surg*. 2008;34:789–795.
9. Klyce SD, Smolek MK, Maeda N. Keratoconus detection with the KISA% method-another view. *J Cataract Refract Surg*. 2000;26:472–474.
10. Smolek MK, Klyce SD. Current keratoconus detection methods compared with a neural network approach. *Invest Ophthalmol Vis Sci*. 1997;38:2290–2299.
11. Rabinowitz YS, McDonnell PJ. Computer-assisted corneal topography in keratoconus. *Refract Corneal Surg*. 1989;5: 400–408.
12. Klyce SD, Karon MD, Smolek MK. Screening patients with the corneal navigator. *J Refract Surg*. 2005;21:S617–S622.
13. Maeda N, Klyce SD, Smolek MK. Neural network classification of corneal topography. Preliminary demonstration. *Invest Ophthalmol Vis Sci*. 1995;36:1327–1335.
14. Klyce SD. Chasing the suspect: keratoconus. *Br J Ophthalmol*. 2009;93(7);845–7.
15. Ambrosio R, Jr., Alonso RS, Luz A. Coca Velarde LG. Corneal-thickness spatial profile and corneal-volume distribution: tomographic indices to detect keratoconus. *J Cataract Refract Surg*. 2006;32:1851–1859.
16. Buhren J, Kook D, Yoon G, Kohnen T. Detection of subclinical keratoconus by using corneal anterior and posterior surface aberrations and thickness spatial profiles. *Invest Ophthalmol Vis Sci*. 2010;51:3424–3432.
17. Buhren J, Kuhne C, Kohnen T. Defining subclinical keratoconus using corneal first-surface higher-order aberrations. *Am J Ophthalmol*. 2007;143:381–389.
18. Jafri B, Li X, Yang H, Rabinowitz YS. Higher order wavefront aberrations and topography in early and suspected keratoconus. *J Refract Surg*. 2007;23:774–781.
19. Zadnik K, Steger-May K, Fink BA, et al. Between-eye asymmetry in keratoconus. *Cornea*. 2002;21:671–679.
20. Rabinowitz YS, Nesburn AB, McDonnell PJ. Videokeratography of the fellow eye in unilateral keratoconus. *Ophthalmology*. 1993;100:181–186.
21. Holland DR, Maeda N, Hannush SB, et al. Unilateral keratoconus. Incidence and quantitative topographic analysis. *Ophthalmology*. 1997;104:1409–1413.
22. Li X, Rabinowitz YS, Rasheed K, Yang H. Longitudinal study of the normal eyes in unilateral keratoconus patients. *Ophthalmology*. 2004;111:440–446.
23. Saad A, Gatinel D. Topographic and tomographic properties of forme fruste keratoconus corneas. *Invest Ophthalmol Vis Sci*. 51:5546–5555.
24. Amsler M. The "forme fruste" of keratoconus (in German). *Wien Klin Wochenschr*. 1961;73:842–843.
25. Jacobs DS, Dohlman CH. Is keratoconus genetic? *Int Ophthalmol Clin*. 1993;33:249–60.
26. Wang Y, Rabinowitz YS, Rotter JI, Yang H. Genetic epidemiological study of keratoconus: evidence for major gene determination. *Am J Med Genet*. 2000;93:403–409.
27. Rabinowitz YS, Maumenee IH, Lundergan MK, et al. Molecular genetic analysis in autosomal dominant keratoconus. *Cornea*. 1992;11:302–308.
28. Muftuoglu O, Erdem U. Evaluation of internal refraction with the optical path difference scan. *Ophthalmology*. 2008;115: 57–66.
29. Buscemi P. Clinical applications of the OPD-Scan wavefront aberrometer/corneal topographer. *J Refract Surg*. 2002;18: S385–S388.
30. MacRae S, Fujieda M. Slit skiascopic-guided ablation using the Nidek laser. *J Refract Surg*. 2000;16:S576–S580.
31. Rabinowitz YS, Rasheed K. KISA% index: a quantitative videokeratography algorithm embodying minimal topographic criteria for diagnosing keratoconus. *J Cataract Refract Surg*. 1999;25:1327–1335.
32. Copeman PW. Eczema and keratoconus. *Br Med J*. 1965;2: 977–979.
33. Karseras AG, Ruben M. Aetiology of keratoconus. *Br J Ophthalmol*. 1976;60:522–525.
34. McMonnies CW. Keratectasia, rubbing, yoga, weightlifting, and intraocular pressure. *Cornea*. 2010;29:952–953
35. McMonnies CW. Abnormal rubbing and keratectasia. *Eye Contact Lens*. 2007;33:265–271.
36. Diniz CM, Tzelikis PF, Rodrigues Junior A, et al. [Unilateral keratoconus associated with continual eye rubbing due to nasolacrimal obstruction–case report]. *Arq Bras Oftalmol*. 2005;68:122–125.
37. Ioannidis AS, Speedwell L, Nischal KK. Unilateral keratoconus in a child with chronic and persistent eye rubbing. *Am J Ophthalmol*. 2005;139:356–357.

38. Wang L, Santaella RM, Booth M, Koch DD. Higher-order aberrations from the internal optics of the eye. *J Cataract Refract Surg*. 2005;31:1512–1519.

39. Alio JL, Shabayek MH. Corneal higher order aberrations: a method to grade keratoconus. *J Refract Surg*. 2006;22:539–545.

40. Lim L, Wei RH, Chan WK, Tan DT. Evaluation of higher order ocular aberrations in patients with keratoconus. *J Refract Surg*. 2007;23:825–828.

41. Nakagawa T, Maeda N, Kosaki R, et al. Higher-order aberrations due to the posterior corneal surface in patients with keratoconus. *Invest Ophthalmol Vis Sci*. 2009;50:2660–2665.

42. Visser N, Berendschot TT, Verbakel F, et al. Evaluation of the comparability and repeatability of four wavefront aberrometers. *Invest Ophthalmol Vis Sci*. 2011;52:1302–1311.

43. Smolek MK, Klyce SD. Goodness-of-prediction of Zernike polynomial fitting to corneal surfaces. *J Cataract Refract Surg*. 2005;31(12):2350–2355.

44. Thibos LN, Hong X, Bradley A, Cheng X. Statistical variation of aberration structure and image quality in a normal population of healthy eyes. *J Opt Soc Am A Opt Image Sci Vis*. 2002; 19(12):2329–2348.

Appendix

$$DA23 = a - 0.575 \times (ZC_1^{-1}) + 0.216 \times (ZC_2^{2}) - 0.793 \times (ZC_3^{3}) - 0.206 \times (ZC_4^{0}) - 0.790 \times (ZC_5^{-3}) - 0.005 \times (ZC_5^{1}) + 1.114 \times (ZC_6^{4}) + 1.549 \times (ZC_6^{6})$$

$$FC = b - 0.576 \times (ZC_1^{-1}) - 0.294 \times (ZC_2^{0}) + 0.289 \times (ZC_2^{2}) - 0.226 \times (ZC_3^{-3}) - 0.387 \times (ZC_3^{3}) + 0.286 \times (ZC_4^{-4}) + 0.239 \times (ZC_4^{-2}) - 0.940 \times (ZC_4^{2}) - 0.934 \times (ZC_5^{-3}) - 1.026 \times (ZC_5^{-1}) + 0.905 \times (ZC_6^{4}) + 2.297 \times (ZC_6^{6}) + 0.304 \times (\text{Corneal Coma RMS}) + 0.325 \times (\text{Corneal Trefoil RMS})$$

$$FT = c + 0.442 \times (ZO_1^{-1}) - 0.685 \times (ZO_1^{1}) - 0.456 \times (ZO_3^{-3}) - 1.314 \times (ZO_3^{-1}) + 0.246 \times (ZO_3^{1}) - 0.471 \times (ZO_3^{3}) - 0.575 \times (ZO_4^{-4}) + 0.693 \times (ZO_4^{-2}) - 0.186 \times (ZO_4^{0}) - 0.474 \times (ZO_5^{-3}) + 0.798 \times (ZO_6^{-2}) + 0.819 \times (ZO_6^{0}) + 1.063 \times (ZO_6^{4}) + 0.602 \times (\text{Ocular Coma RMS})$$

$$FCT = d - 0.372 \times (ZO_1^{1}) - 0.820 \times (ZO_3^{-1}) - 0.612 \times (ZO_4^{-4}) - 0.359 \times (ZO_4^{0}) + 1.518 \times (ZO_4^{2}) + 0.780 \times (ZO_6^{0}) - 0.175 \times (ZO_6^{6}) + 0.290 \times (\text{Ocular Coma RMS}) - 0.138 \times (ZC_2^{-2}) - 0.315 \times (ZC_2^{0}) - 0.131 \times (ZC_3^{-3}) - 0.400 \times (ZC_3^{-3}) + 0.474 \times (ZC_4^{-4}) + 0.533 \times (ZC_4^{-2}) - 1.396 \times (ZC_4^{2}) - 0.736 \times (ZC_5^{-3}) + 1.502 \times (ZC_6^{-6}) + 0.322 \times (ZC_6^{-2}) - 0.569 \times (ZC_6^{2}) + 1.241 \times (ZC_6^{4}) + 2.611 \times (ZC_6^{6}) + 0.291 \times (\text{Corneal Spherical RMS})$$

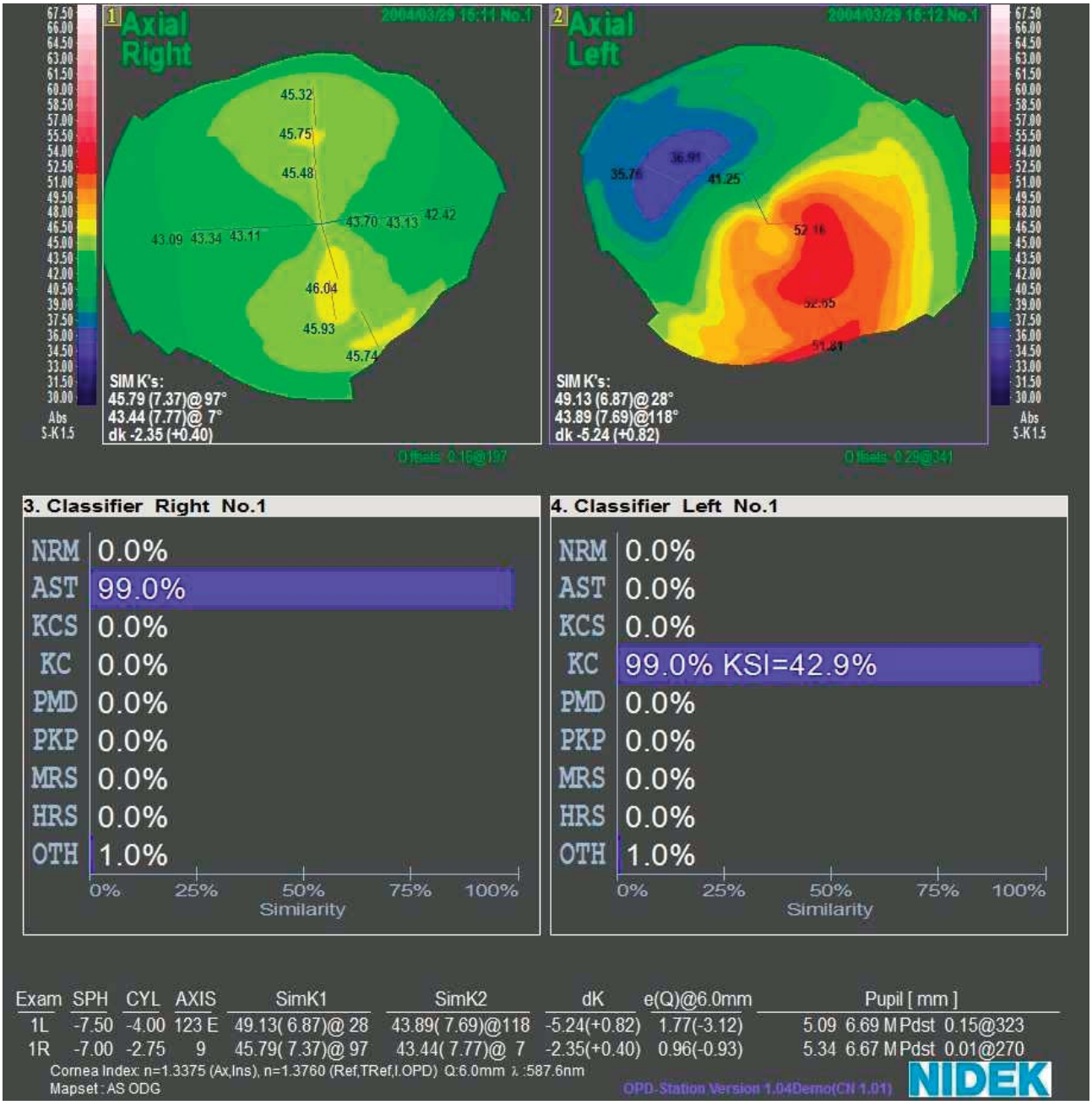
1 Axial Right
2004/03/29 15:11 No.1
45.32
45.75
45.48
43.09 43.34 43.11
43.70 43.13 42.42
46.04
45.93
45.74
SIM K's:
45.79 (7.37)@ 97°
43.44 (7.77)@ 7°
dk -2.35 (+0.40)
2 Axial Left
2004/03/29 15:12 No.1
35.76
36.91
41.25
SIM K's:
49.13 (6.87)@ 28°
43.89 (7.69)@118°
dk -5.24 (+0.82)
Abs
S-K1.5
3. Classifier Right No.1
NRM 0.0%
AST 99.0%
KCS 0.0%
KC 0.0%
PMD 0.0%
PKP 0.0%
MRS 0.0%
HRS 0.0%
OTH 1.0%
0% 25% 50% 75% 100%
Similarity
4. Classifier Left No.1
NRM 0.0%
AST 0.0%
KCS 0.0%
KC 99.0% KSI=42.9%
PMD 0.0%
PKP 0.0%
MRS 0.0%
HRS 0.0%
OTH 1.0%
0% 25% 50% 75% 100%
Similarity
Exam SPH CYL AXIS SimK1 SimK2 dK e(Q)@6.0mm Pupil [mm]
1L -7.50 -4.00 123 E 49.13(6.87)@ 28 43.89(7.69)@118 -5.24(+0.82) 1.77(-3.12) 5.09 6.69 MPdst 0.15@323
1R -7.00 -2.75 9 45.79(7.37)@ 97 43.44(7.77)@ 7 -2.35(+0.40) 0.96(-0.93) 5.34 6.67 MPdst 0.01@270
Cornea Index: n=1.3375 (Ax,Ins), n=1.3760 (Ref,TRef,I.OPD) Q:6.0mm λ :587.6nm
Mapset : AS ODG
OPD-Station Version 1.04Demo(CN 1.01)
NIDEK

Figure A1.

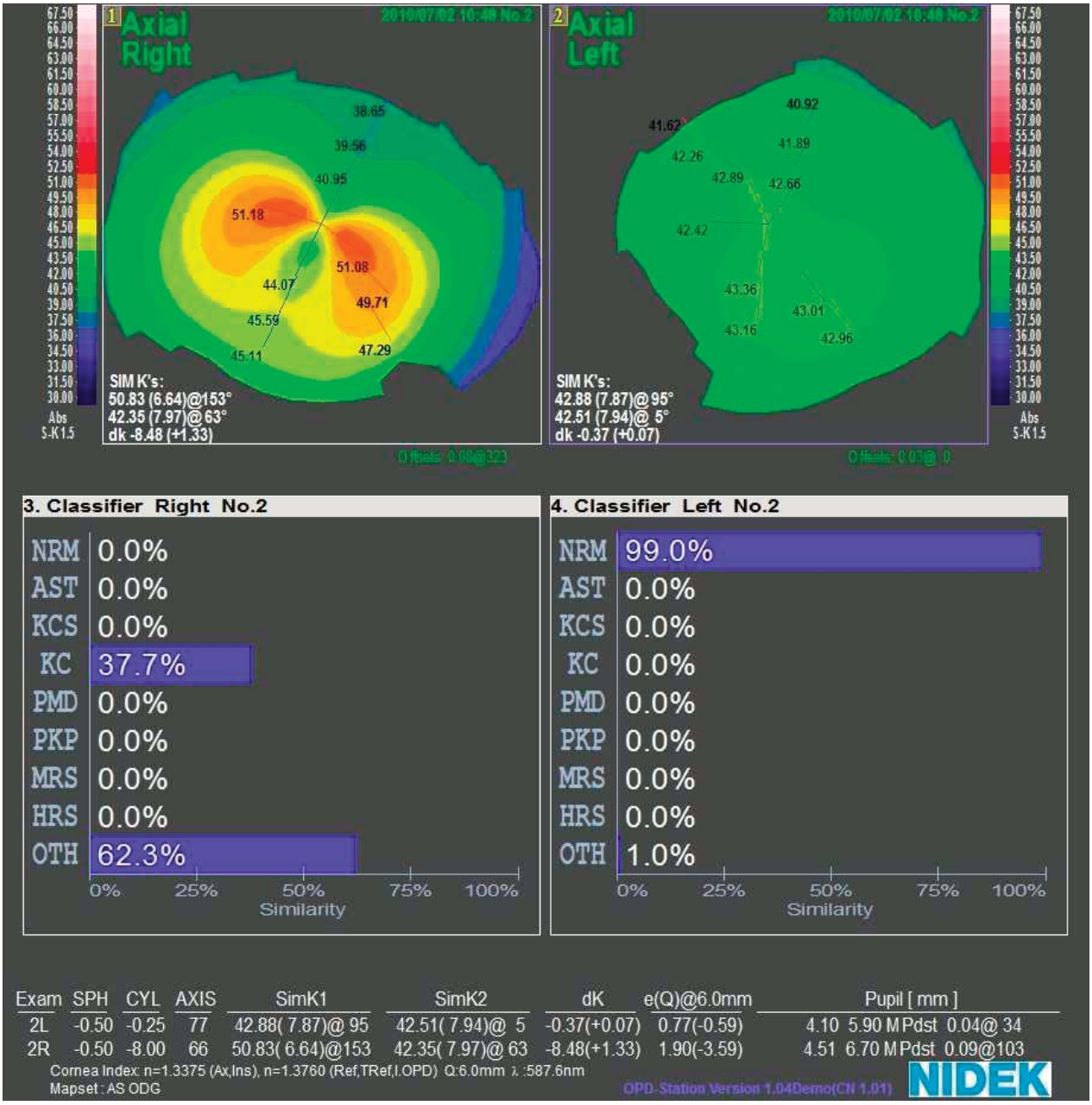
1 Axial Right
2010/07/02 10:48 No.2
38.65
39.56
40.95
51.18
51.08
44.07
49.71
45.59
45.11
47.29
SIM K's:
50.83 (6.64)@153°
42.35 (7.97)@ 63°
dk -8.48 (+1.33)
2 Axial Left
2010/07/02 10:48 No.2
40.92
41.62
41.89
42.26
42.89
42.66
42.42
43.36
43.01
43.16
42.96
SIM K's:
42.88 (7.87)@ 95°
42.51 (7.94)@ 5°
dk -0.37 (+0.07)
Abs
5-K1.5
3. Classifier Right No.2
NRM 0.0%
AST 0.0%
KCS 0.0%
KC 37.7%
PMD 0.0%
PKP 0.0%
MRS 0.0%
HRS 0.0%
OTH 62.3%
0% 25% 50% 75% 100%
Similarity
4. Classifier Left No.2
NRM 99.0%
AST 0.0%
KCS 0.0%
KC 0.0%
PMD 0.0%
PKP 0.0%
MRS 0.0%
HRS 0.0%
OTH 1.0%
0% 25% 50% 75% 100%
Similarity
Exam SPH CYL AXIS SimK1 SimK2 dK e(Q)@6.0mm Pupil [mm]
2L -0.50 -0.25 77 42.88(7.87)@ 95 42.51(7.94)@ 5 -0.37(+0.07) 0.77(-0.59) 4.10 5.90 M Pdst 0.04@ 34
2R -0.50 -8.00 66 50.83(6.64)@153 42.35(7.97)@ 63 -8.48(+1.33) 1.90(-3.59) 4.51 6.70 M Pdst 0.09@103
Cornea Index: n=1.3375 (Ax,Ins), n=1.3760 (Ref,TRef,I.OPD) Q:6.0mm λ :587.6nm
Mapset : AS ODG
OPD-Station Version 1.04Demo(CN 1.01)
NIDEK

FIGURE A2.

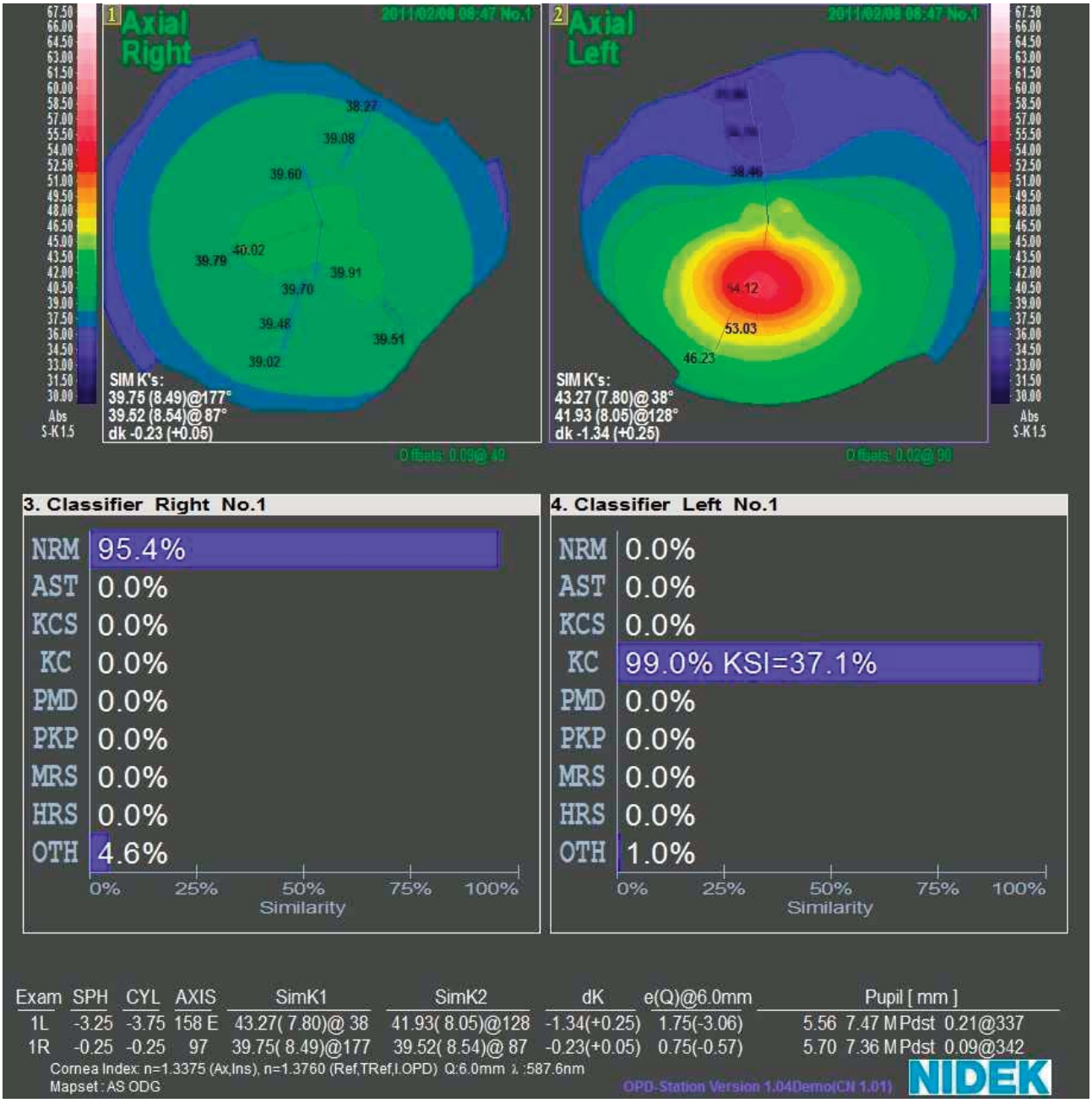
1 Axial Right
2011/02/08 08:47 No.1
38.27
39.08
39.60
40.02
39.79
39.91
39.70
39.48
39.51
39.02
SIM K's:
39.75 (8.49)@177°
39.52 (8.54)@ 87°
dk -0.23 (+0.05)
2 Axial Left
2011/02/08 08:47 No.1
38.46
54.12
53.03
46.23
SIM K's:
43.27 (7.80)@ 38°
41.93 (8.05)@128°
dk -1.34 (+0.25)
Abs
S-K1.5
3. Classifier Right No.1
NRM 95.4%
AST 0.0%
KCS 0.0%
KC 0.0%
PMD 0.0%
PKP 0.0%
MRS 0.0%
HRS 0.0%
OTH 4.6%
0% 25% 50% 75% 100%
Similarity
4. Classifier Left No.1
NRM 0.0%
AST 0.0%
KCS 0.0%
KC 99.0% KSI=37.1%
PMD 0.0%
PKP 0.0%
MRS 0.0%
HRS 0.0%
OTH 1.0%
0% 25% 50% 75% 100%
Similarity
Exam SPH CYL AXIS SimK1 SimK2 dK e(Q)@6.0mm Pupil [mm]
1L -3.25 -3.75 158 E 43.27(7.80)@ 38 41.93(8.05)@128 -1.34(+0.25) 1.75(-3.06) 5.56 7.47 M Pdst 0.21@337
1R -0.25 -0.25 97 39.75(8.49)@177 39.52(8.54)@ 87 -0.23(+0.05) 0.75(-0.57) 5.70 7.36 M Pdst 0.09@342
Cornea Index: n=1.3375 (Ax,Ins), n=1.3760 (Ref,TRef,I.OPD) Q:6.0mm λ :587.6nm
Mapset : AS ODG
OPD-Station Version 1.04Demo(CN 1.01)
NIDEK

FIGURE A3.

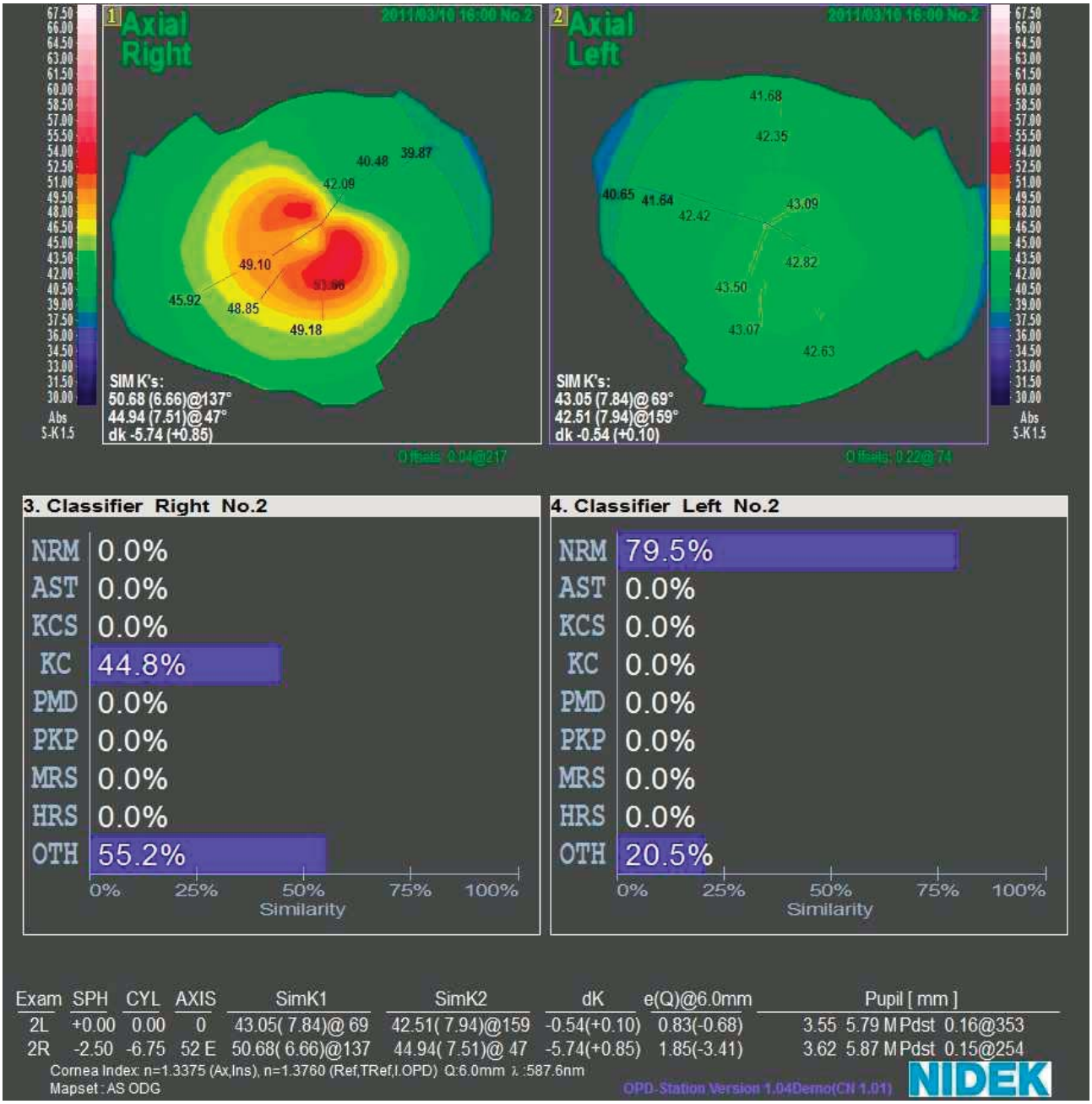
1 Axial Right
2011/03/10 16:00 No.2
40.48
39.87
42.09
49.10
45.92
48.85
49.18
SIM K's:
50.68 (6.66)@137°
44.94 (7.51)@ 47°
dk -5.74 (+0.85)
2 Axial Left
2011/03/10 16:00 No.2
41.68
42.35
40.65
41.84
42.42
43.09
42.82
43.50
43.07
42.63
SIM K's:
43.05 (7.84)@ 69°
42.51 (7.94)@159°
dk -0.54 (+0.10)
Abs
S-K1.5
3. Classifier Right No.2
NRM 0.0%
AST 0.0%
KCS 0.0%
KC 44.8%
PMD 0.0%
PKP 0.0%
MRS 0.0%
HRS 0.0%
OTH 55.2%
0% 25% 50% 75% 100%
Similarity
4. Classifier Left No.2
NRM 79.5%
AST 0.0%
KCS 0.0%
KC 0.0%
PMD 0.0%
PKP 0.0%
MRS 0.0%
HRS 0.0%
OTH 20.5%
0% 25% 50% 75% 100%
Similarity
Exam SPH CYL AXIS SimK1 SimK2 dK e(Q)@6.0mm Pupil [mm]
2L +0.00 0.00 0 43.05(7.84)@ 69 42.51(7.94)@159 -0.54(+0.10) 0.83(-0.68) 3.55 5.79 M Pdst 0.16@353
2R -2.50 -6.75 52 E 50.68(6.66)@137 44.94(7.51)@ 47 -5.74(+0.85) 1.85(-3.41) 3.62 5.87 M Pdst 0.15@254
Cornea Index: n=1.3375 (Ax,Ins), n=1.3760 (Ref,TRef,I.OPD) Q:6.0mm λ :587.6nm
Mapset : AS ODG
OPD-Station Version 1.04Demo(CN 1.01)
NIDEK

FIGURE A4.

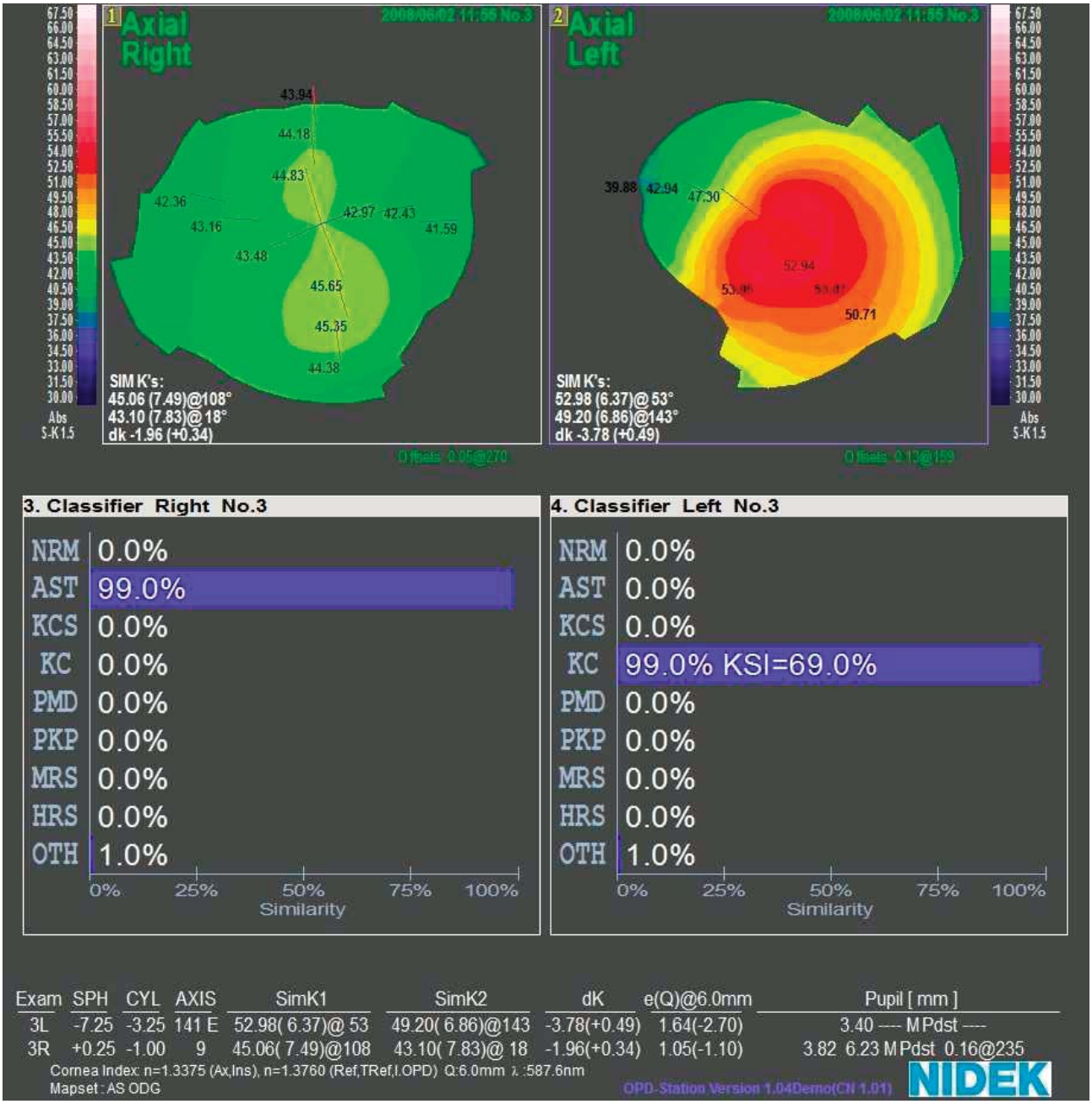
1 Axial Right
2008/06/02 11:55 No.3
43.94
44.18
44.83
42.36
43.16
42.97
42.43
41.59
43.48
45.65
45.35
44.38
SIM K's:
45.06 (7.49)@108°
43.10 (7.83)@ 18°
dk -1.96 (+0.34)
2 Axial Left
2008/06/02 11:55 No.3
39.88
42.94
47.30
52.94
50.71
SIM K's:
52.98 (6.37)@ 53°
49.20 (6.86)@143°
dk -3.78 (+0.49)
Abs
S-K1.5
3. Classifier Right No.3
NRM 0.0%
AST 99.0%
KCS 0.0%
KC 0.0%
PMD 0.0%
PKP 0.0%
MRS 0.0%
HRS 0.0%
OTH 1.0%
0% 25% 50% 75% 100%
Similarity
4. Classifier Left No.3
NRM 0.0%
AST 0.0%
KCS 0.0%
KC 99.0% KSI=69.0%
PMD 0.0%
PKP 0.0%
MRS 0.0%
HRS 0.0%
OTH 1.0%
0% 25% 50% 75% 100%
Similarity
Exam SPH CYL AXIS SimK1 SimK2 dK e(Q)@6.0mm Pupil [mm]
3L -7.25 -3.25 141 E 52.98(6.37)@ 53 49.20(6.86)@143 -3.78(+0.49) 1.64(-2.70) 3.40 ---- MPdst ----
3R +0.25 -1.00 9 45.06(7.49)@108 43.10(7.83)@ 18 -1.96(+0.34) 1.05(-1.10) 3.82 6.23 MPdst 0.16@235
Cornea Index: n=1.3375 (Ax,Ins), n=1.3760 (Ref,TRef,I.OPD) Q:6.0mm λ :587.6nm
Mapset : AS ODG
OPD-Station Version 1.04Demo(CN 1.01)
NIDEK

FIGURE A5.

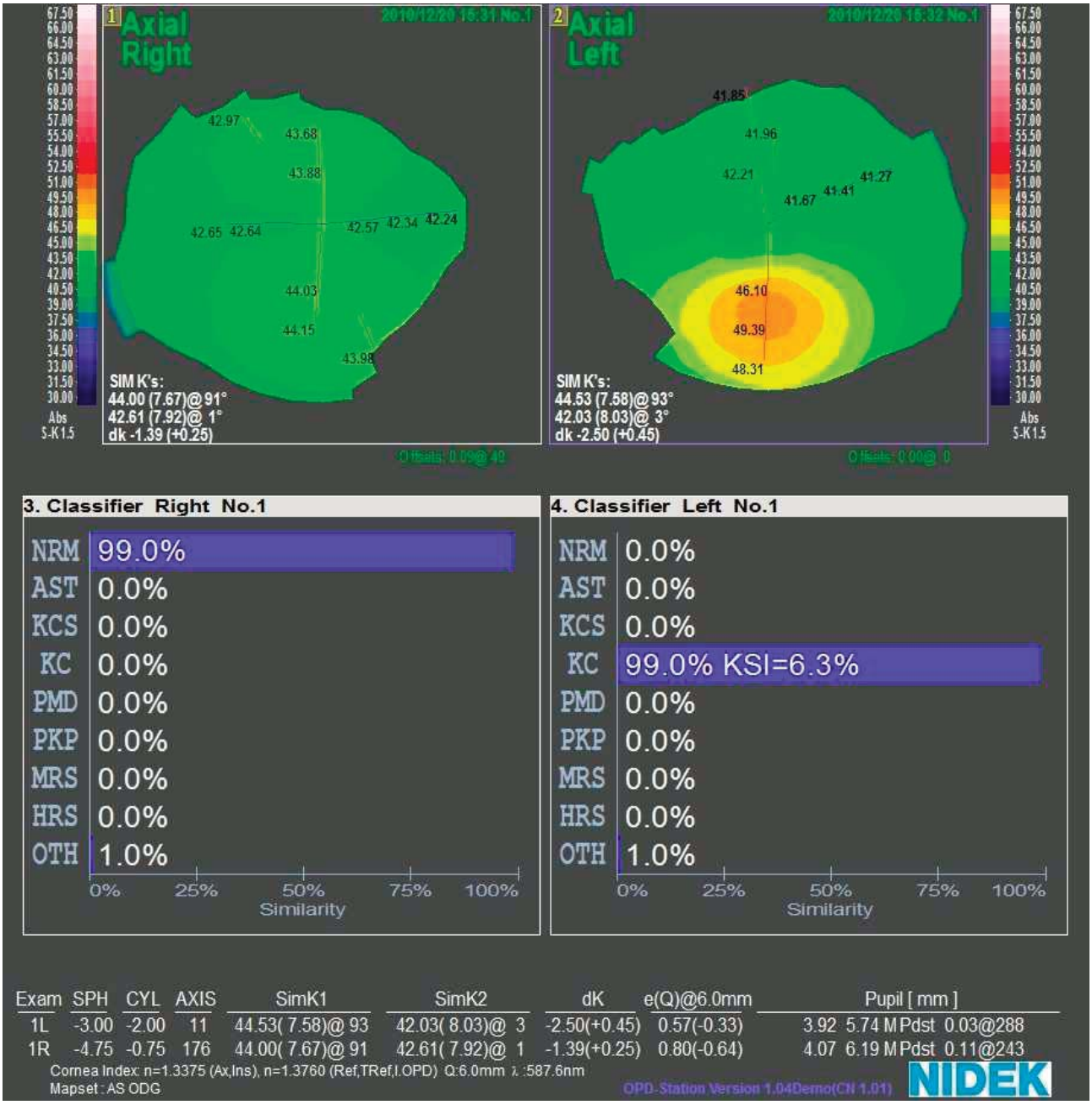
1 Axial Right
2010/12/20 15:31 No.1
42.97
43.68
43.88
42.65 42.64
42.57 42.34 42.24
44.03
44.15
43.98
SIM K's:
44.00 (7.67)@ 91°
42.61 (7.92)@ 1°
dk -1.39 (+0.25)
2 Axial Left
2010/12/20 15:32 No.1
41.85
41.96
42.21
41.27
41.67
41.41
46.10
49.39
48.31
SIM K's:
44.53 (7.58)@ 93°
42.03 (8.03)@ 3°
dk -2.50 (+0.45)
Abs
S-K1.5
3. Classifier Right No.1
NRM 99.0%
AST 0.0%
KCS 0.0%
KC 0.0%
PMD 0.0%
PKP 0.0%
MRS 0.0%
HRS 0.0%
OTH 1.0%
0% 25% 50% 75% 100%
Similarity
4. Classifier Left No.1
NRM 0.0%
AST 0.0%
KCS 0.0%
KC 99.0% KSI=6.3%
PMD 0.0%
PKP 0.0%
MRS 0.0%
HRS 0.0%
OTH 1.0%
0% 25% 50% 75% 100%
Similarity
Exam SPH CYL AXIS SimK1 SimK2 dK e(Q)@6.0mm Pupil [mm]
1L -3.00 -2.00 11 44.53(7.58)@ 93 42.03(8.03)@ 3 -2.50(+0.45) 0.57(-0.33) 3.92 5.74 MPdst 0.03@288
1R -4.75 -0.75 176 44.00(7.67)@ 91 42.61(7.92)@ 1 -1.39(+0.25) 0.80(-0.64) 4.07 6.19 MPdst 0.11@243
Cornea Index: n=1.3375 (Ax,Ins), n=1.3760 (Ref,TRef,I.OPD) Q:6.0mm λ :587.6nm
Mapset : AS ODG
OPD-Station Version 1.04Demo(CN 1.01)
NIDEK

Figure A6.

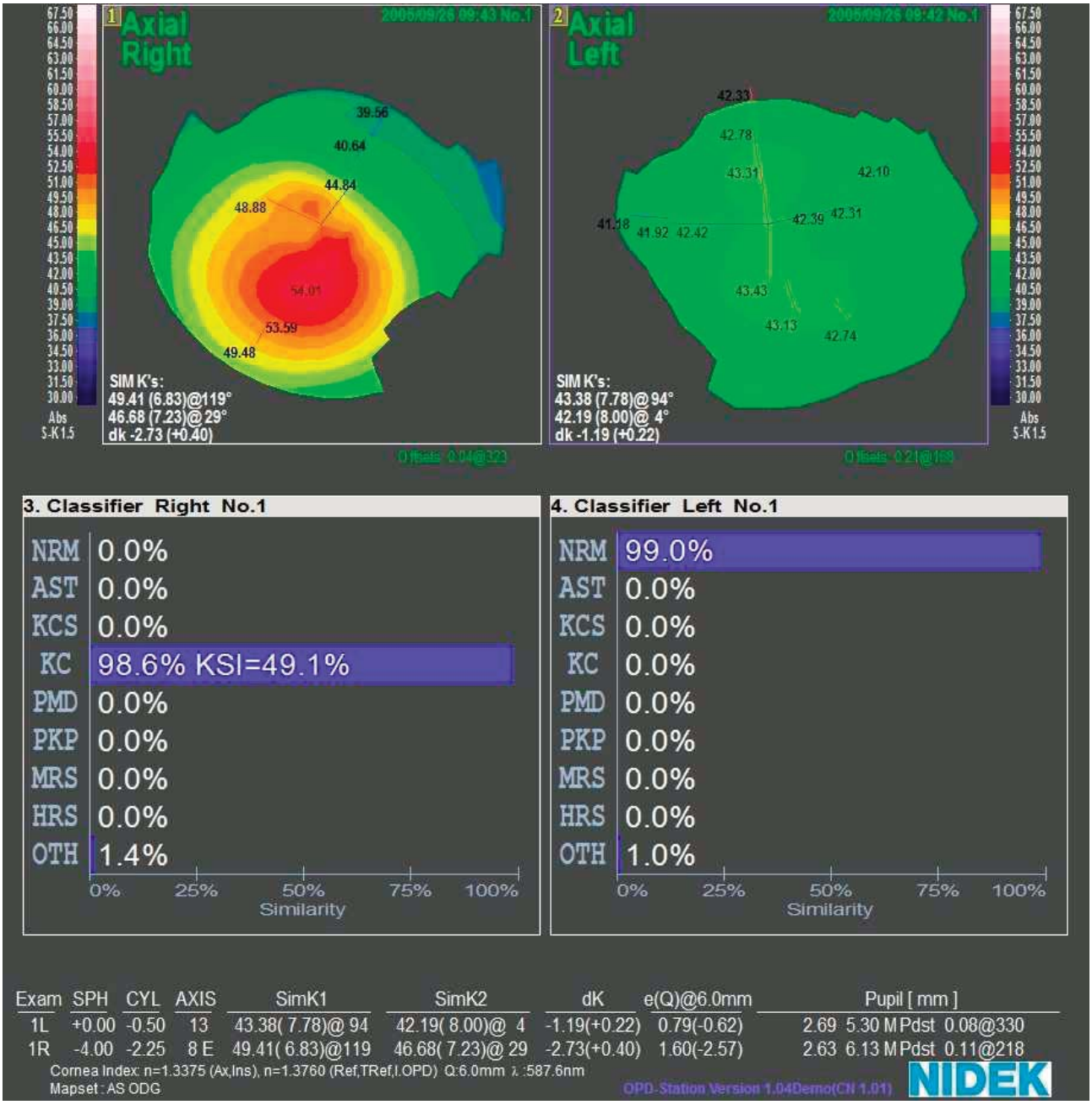
1 Axial Right
39.56
40.64
44.84
48.88
54.01
53.59
49.48
SIM K's:
49.41 (6.83)@119°
46.68 (7.23)@ 29°
dk -2.73 (+0.40)
2 Axial Left
42.33
42.78
43.31
42.10
41.58
41.92
42.42
42.39
42.31
43.43
43.13
42.74
SIM K's:
43.38 (7.78)@ 94°
42.19 (8.00)@ 4°
dk -1.19 (+0.22)
Abs
S-K1.5
3. Classifier Right No.1
NRM 0.0%
AST 0.0%
KCS 0.0%
KC 98.6% KSI=49.1%
PMD 0.0%
PKP 0.0%
MRS 0.0%
HRS 0.0%
OTH 1.4%
0% 25% 50% 75% 100%
Similarity
4. Classifier Left No.1
NRM 99.0%
AST 0.0%
KCS 0.0%
KC 0.0%
PMD 0.0%
PKP 0.0%
MRS 0.0%
HRS 0.0%
OTH 1.0%
0% 25% 50% 75% 100%
Similarity
Exam SPH CYL AXIS SimK1 SimK2 dK e(Q)@6.0mm Pupil [mm]
1L +0.00 -0.50 13 43.38(7.78)@ 94 42.19(8.00)@ 4 -1.19(+0.22) 0.79(-0.62) 2.69 5.30 M Pdst 0.08@330
1R -4.00 -2.25 8 E 49.41(6.83)@119 46.68(7.23)@ 29 -2.73(+0.40) 1.60(-2.57) 2.63 6.13 M Pdst 0.11@218
Cornea Index: n=1.3375 (Ax,Ins), n=1.3760 (Ref,TRef,I.OPD) Q:6.0mm λ :587.6nm
Mapset : AS ODG
OPD-Station Version 1.04Demo(CN 1.01)
NIDEK

FIGURE A7.

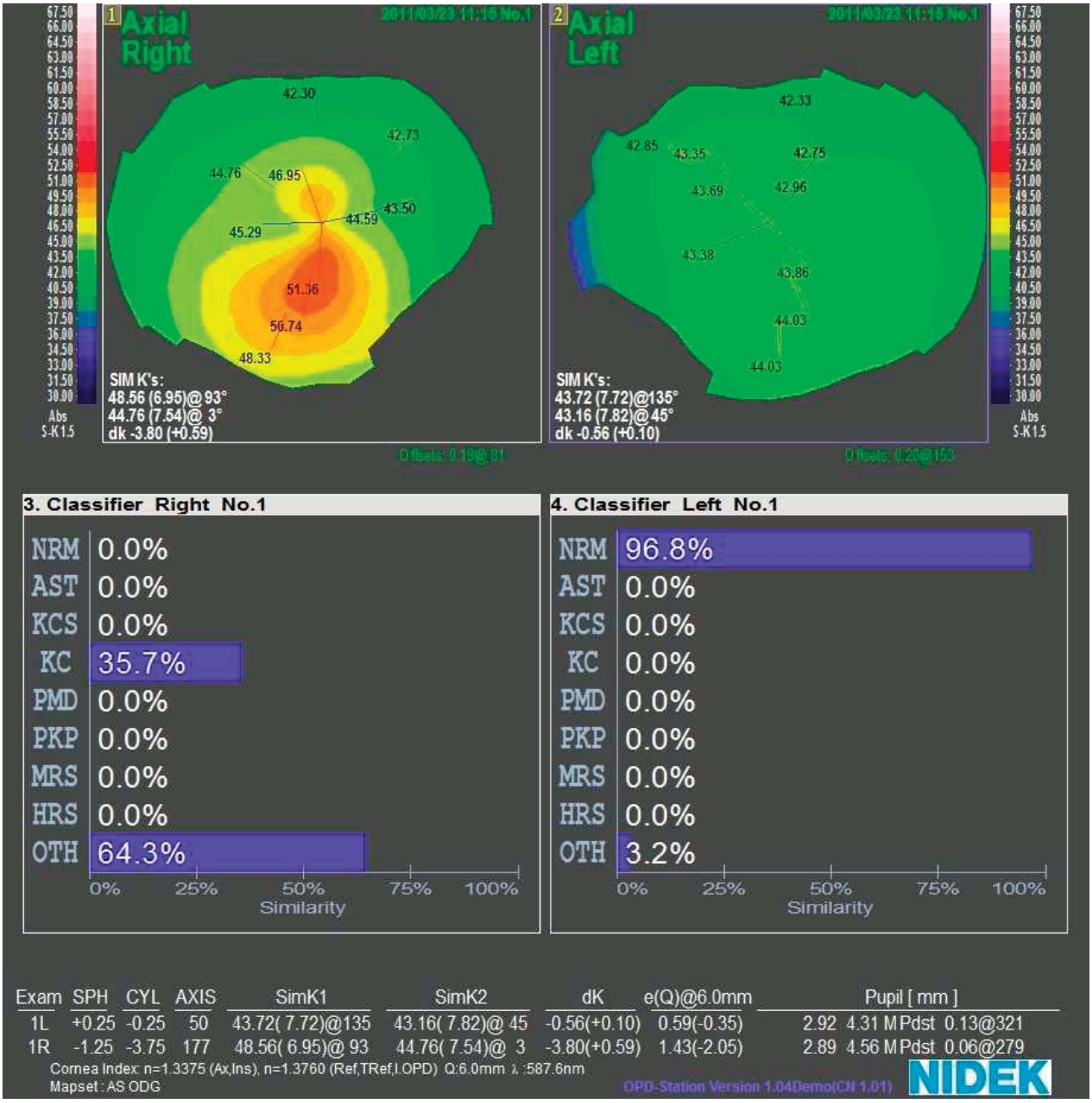
1 Axial Right
2011/03/23 11:15 No.1
42.30
42.73
44.76
46.95
43.50
44.59
45.29
51.36
56.74
48.33
SIM K's:
48.56 (6.95)@ 93°
44.76 (7.54)@ 3°
dk -3.80 (+0.59)
2 Axial Left
2011/03/23 11:15 No.1
42.33
42.85
43.35
42.75
43.69
42.96
43.38
43.86
44.03
44.03
SIM K's:
43.72 (7.72)@135°
43.16 (7.82)@ 45°
dk -0.56 (+0.10)
Abs
S-K1.5
3. Classifier Right No.1
NRM 0.0%
AST 0.0%
KCS 0.0%
KC 35.7%
PMD 0.0%
PKP 0.0%
MRS 0.0%
HRS 0.0%
OTH 64.3%
0% 25% 50% 75% 100%
Similarity
4. Classifier Left No.1
NRM 96.8%
AST 0.0%
KCS 0.0%
KC 0.0%
PMD 0.0%
PKP 0.0%
MRS 0.0%
HRS 0.0%
OTH 3.2%
0% 25% 50% 75% 100%
Similarity
Exam SPH CYL AXIS SimK1 SimK2 dK e(Q)@6.0mm Pupil [mm]
1L +0.25 -0.25 50 43.72(7.72)@135 43.16(7.82)@ 45 -0.56(+0.10) 0.59(-0.35) 2.92 4.31 M Pdst 0.13@321
1R -1.25 -3.75 177 48.56(6.95)@ 93 44.76(7.54)@ 3 -3.80(+0.59) 1.43(-2.05) 2.89 4.56 M Pdst 0.06@279
Cornea Index: n=1.3375 (Ax,Ins), n=1.3760 (Ref,TRef,I.OPD) Q:6.0mm λ :587.6nm
Mapset : AS ODG
OPD-Station Version 1.04Demo(CN 1.01)
NIDEK

Figure A8.